JOURNAL OF THE KOREAN ASTRONOMICAL SOCIETY
26: 13 ~ 32, 1993

BVI SURFACE PHOTOMETRY OF FOUR SPIRAL GALAXIES

ANN, HONG BAE
Department of Earth Sciences, Pusan National University, Pusan 609-735
AND
PARK, NAM GYU
Korea Astronomical Observatory
(Received March 25, 1993; Accepted April 20, 1993)

ABSTRACT

We have conducted BVI photographic surface photometry of four spiral galaxies NGC1087, NGC2715, NGC2844 and NGC3593, by making use of the Kiso Schmidt plates. Detailed examination of the morphological properties of the galaxies using isophotal maps and luminosity profiles showed that all the program galaxies have some peculiarities in their luminosity distributions. NGC1087 and NGC2715 have extremely small nuclei with inner rings which contain several bright HII regions. NGC2844 has a very large bulge whose luminosity dominates over the disk luminosity in all the radii. The I-band luminosity profile of NGC3593 shows shallower gradient than B- and V-band profiles. We were able to successfully decompose the luminosity profile into a bulge following de Vaucouleurs $r^{1/4}$-law and an exponential disk only for NGC 3953. Other galaxies have more complicated luminosit profiles.

Key Words: galaxies, photometry, structure.

I. INTRODUCTION

Photographic surface photometry of galaxies has been one of the major branch of extragalactic studies since Hubble's pioneering work in the early 1930s. Most of the current knowledge about the structure of galaxies came from the analysis of the photographic plates. The photographic surface photometry of galaxies has been done highly automatically since the introduction of digitizing machines, such as PDS, in 1970s. Because the errors of the photographic photometry have been significantly reduced by employing the automatic reduction procedure, the photographic surface photometry of galaxies still plays an important roll in the extragalactic research. One good example is the Photometric Atlas of Northern Bright Galaxies (Kodaira et al. 1990).

Although CCDs are superior in many aspects to photographic plates for astronomical observations, it is quite reasonable to use existing photographic plates in many fields of observational astronomy. One of the best sources of plates is the plate library of the Kiso Observatory since most of the plates are deep enough to be used for detailed surface photometry of galaxies and for searching faint objects such as quasars and faint galaxies. Besides the survey plates catalogued by Kodaira et al. (1990), there are a number of deep plates in multi-wavebands.

There have been several works on the galaxy surface photometry using Kiso Schmidt plates (Watanabe et al. 1982; Okamura et al. 1984 ; Watanabe et al. 1985; Ann 1986, 1987; Kodaira et al. 1990). The basic tool to conduct surface photometry in the above papers was a software called SPIRAL (Surface Photometry Interactive Reduction and Analysis Library), which was developed at the Kiso Observatory for FACOMS-3500 computer, but recently it is implemented on the SUN workstations to be coupled with IRAF (Hamabe 1992).

The purpose of the present study is to use the existing Kiso Schmidt plates in order to investigate the physical morphology of the four spiral galaxies. We will give a very brief guide to SPIRAL/IRAF for the novices to it. In §II, we describe the observational material and the basic reduction procedures. The morphology of the galaxies based on the two-dimensional luminosity distribution is described in §III and an analysis of the major axis profiles is given in §IV. A brief summary and

Table 1. Fundamental Parameters of the Program Galaxies

NGC	RA	Dec	Type	D (arcmin)	Mag.	A_b	V (km/sec)
1087	$02^h43^m32^s$	-00°42′19″	SAB(rs)c	3.7 x 2.2	11.46	0.11	1519
2715	09^h01m53^s	78°17′15″	SAB(rs)c	4.9 x 1.7	11.79	0.02	1323
2844	$09^h18^m38^s$	40°21′52″	SA(r)a	1.5 x 0.8	13.75	0.00	1486
3593	$11^h11^m59^s$	13°05′28″	SA(s)0/a	5.2 x 1.9	11.86	0.00	628

conclusions of the present study are followed in the last section.

II. OBSERVATION AND DATA REDUCTION

We selected four spiral galaxies NGC1087, NGC2715, NGC2844, and NGC3593 for which deep BVI Kiso Schmidt plates are available as our object. NGC1087 and NGC2715 are late type spirals and NGC2844 and NGC3593 are early type ones whose luminosity distributions are not well known. We present the fundamental data of the program galaxies in Table 1 where all the data are extracted from the on-line NASA Extragalactic Database (NED).

The reduction procedures for the surface photometry of a galaxy consist of several steps such as conversion of photographic density to intensity, background sky subtraction, smoothing, cleaning, and absolute calibration. We performed all the reductions by using SPIRAL/IRAF which was recently installed to SUN workstations. Because the reduction procedure has been described quite a detail (Ann 1986, Ichikawa et al. 1987; Okamura 1988), we will only outline the procedure very briefly. More detailed description of SPIRAL/IRAF will be given elsewhere (Ann 1993).

(a) Plate Measurements

The Kiso plate scale is 62.5 arcsec/mm. We scanned the area of 20mm by 20mm centered on the program galaxy. The scanned areas are four to five times larger than the visible part of the program galaxies, in order to ensure accurate determination of the sky background. It took about one hour to scan the target area with scanning speed of 150 (in PDS units) with Kiso Observatory's PDS 2020GMS. This was possible because of a fast logarithmic amplifier which is five times faster than the original Perkin-Elmer amplifier (Tarusawa et al. 1986). We used a square aperture of 17μm and sampled the data at each 16 μm interval in both x and y directions. This sampling pitch corresponds to one arcsec on the sky and gives a good sampling of data because the mean seeing of the Kiso Observatory is 2-3 arcsec (Kodaira et al. 1990).

For the calibration of the photographic density we scanned the four sets of step wedges which were exposed on the margin of the plate just after galaxy exposure with the same filter and the same exposure time as for the galaxy observation. The scanning area of one set of 15 step wedges was a rectangle of 10 x 120 mm. We used the same aperture and speed for the wedge scan as those for galaxy area but the sampling pitch was 50 μm and 500 μm along the short and long sides of the rectanglc, respectively. With this scanning parameter it took about two minutes to scan one set of 15 step wedges.

(b) Conversion of Density to Intensity and Sky Subtraction

The output of a galaxy scan described in the previous section is a digital array in which each element represents the photographic density at the scanned position. We call this as a density frame. We convert the density frame to intensity frame by using a characteristic curve of each plate. We determined characteristic curve of each plate by fitting the data to a Goad function after rejection of bad data which deviate much from the mean characteristic curve of the other three wedges.

Because the outer parts of galaxies are much fainter than the background sky, the subtraction of background sky is the most critical process in galaxy surface photometry. The effect of sky subtraction on the resulting luminosity profiles of a galaxy was well demonstrated in Mihalas and Binney (1981). In this paper we subtracted the sky background by fitting the values of the whole intensity frame to a two-dimensional polynominal after masking the regions covered by the galaxy itself and other bright objects such as bright stars and neighboring galaxies. The validity of the applied sky subtraction

was checked by visual inspection of the resulting residuals on the image display. We tried from the zeroth order to the fifth order polynominals to fit the sky background but it was found that the first order polynominal gives the best result for all the program galaxies.

After fitting the polynominals to the background sky, we trimmed the intensity frames to smaller sizes to save storage space and easy handling. The size of a galaxy frame was determined by the apparent size of the galaxy. We adopted 256x256 array for NGC1087, NGC2844, and 512x512 array for NGC3593. The relative intensity of a galaxy can be represented as

$$I_{rel}(x,y) = [I(x,y) - I_S(x,y)]\,/\,I_S(x,y),$$

where $I(x,y)$ is the galaxy frame after trimming and $I_S(x,y)$ is fitted sky background intensity. The unit of the relative intensity is the sky brightness whose absolute calibration can be done in various ways.

(c) Smoothing and Cleaning

Because of the low S/N in the outer parts of the galaxy, it is necessary to smooth the relative intensity frame for further analysis of the galaxy. In IRAF package there are several tasks which can be used for smoothing of the image frame. However, it is more convenient to use SMOOTH in SPIRAL because it uses different sizes for the smoothing length for different parts with different S/N. We used variable-width Gaussian beam for smoothing kernel with standard deviation as a threshold.

Because the galactic image is contaminated by foreground stars, we performed cleaning process for the smoothed frames. In the cleaning process, the values of the unwanted pixels are replaced by the values interpolated from the surrounding pixels, by making use of IMEDIT in IRAF. We did not clean the foreground stars far from the galaxtic center because these stars do not affect the luminosity distribution of the galaxies.

(d) Absolute Calibration

The geometric properties of galaxies can be analyzed with uncalibrated sky brightness. However, it is necessary to determine the absolute sky brightness if we we want to derive the photometric parameters in the standard photometric systems because the unit of the relative intensity is sky brightness. There are several ways to perform the absolute calibration but SPIRAL uses the method of curve of growth. We used the Catalog of Longo and de Vaucouleurs (1983) for the determination of sky brightness of all the program galaxies.

One problem in determining the absolute sky brightness from the curve of growth method is the difficulties of correcting the effect of bright field stars (Kodaira et al. 1990). Because some photoelectric photometry was corrected for bright field stars while others were not, there is no easy way to eliminate the effect of contaminated stars. The best way to overcome this problem is to use individual photoelectric magnitudes of several field stars in the galaxy frame, but it is always nearly impossible because most of the field stars are too faint to be observed reliably. This is one of the inevitable sources of uncertainties in photographic surface photometry of galaxies.

III. MORPHOLOGY FROM TWO-DIMENSIONAL LUMINOSITY DISTRIBUTION

We examined the morphological properties of NGC1087, NGC2715, NGC2844, and NGC3593, by using the isophotal maps as shown in Figures 1 - 4, along with density maps on SAOimage which allows easy identification of detailed features. The sizes of the isophotal maps are the same as those of the relative intensity matrix, i.e., each tick in ordinate and abscissa represents 10 arcsec except for the isophotal maps of NGC3593 where the tick interval is 20 arcsec. The intervals between isophotes are 0.5 magnitude and the surface brightness of the outermost isophote is about 3.5 magnitude below the sky brightness except that of NGC3593 in I-band which is 1 magnitude below the sky brightness. In all the isophotal maps, top is to the north and left is to the east.

The isophotal maps of NGC1087 in Figure 1 show that it has a very small nucleus with multiple spiral arms. The spiral arms of NGC1087 are not as bright as those in other Sc galaxies but there are many dust lanes and HII regions. The small elongated feature across the nucleus seems to be a bar whose position angle (PA) and ellipticity are about 110° and 0.5°, respectively. There is an inner ring outside the bar and the spiral arms are connected to this inner ring. Several bright

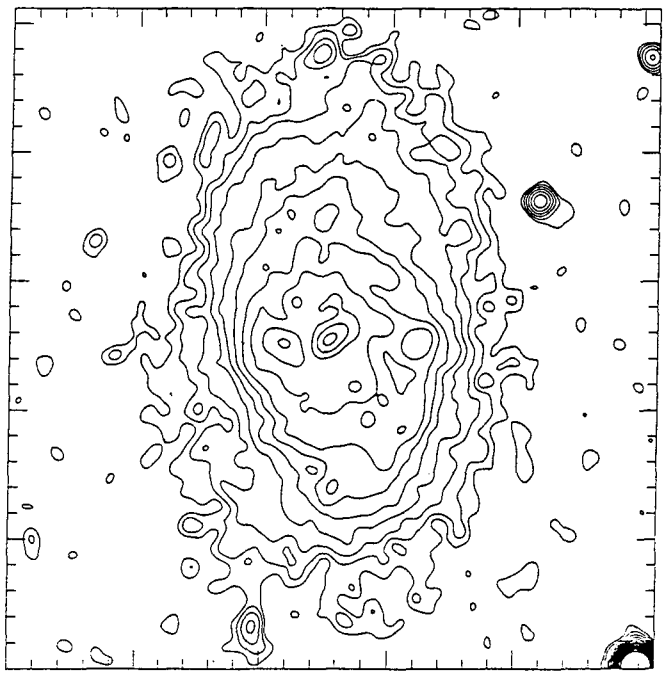

N1087 B

(a)

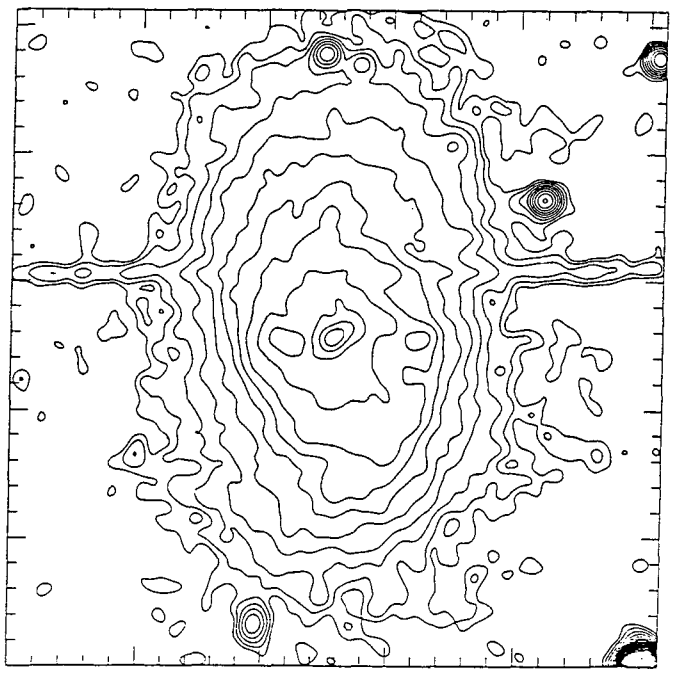

N1087 V

(b)

Fig. 1. Isophotal maps of NGC1087. North is at top and east at left. The intervals of isophotes are 0.5 mag. (a) B-band isophotal map which shows multiple spiral arms and dust lanes. The outermost isophote represents 25 mag/arcsec^2. The central elongated feature is bar. (b) The same for V-band. The horizontally elongated feature is due to plate defect.

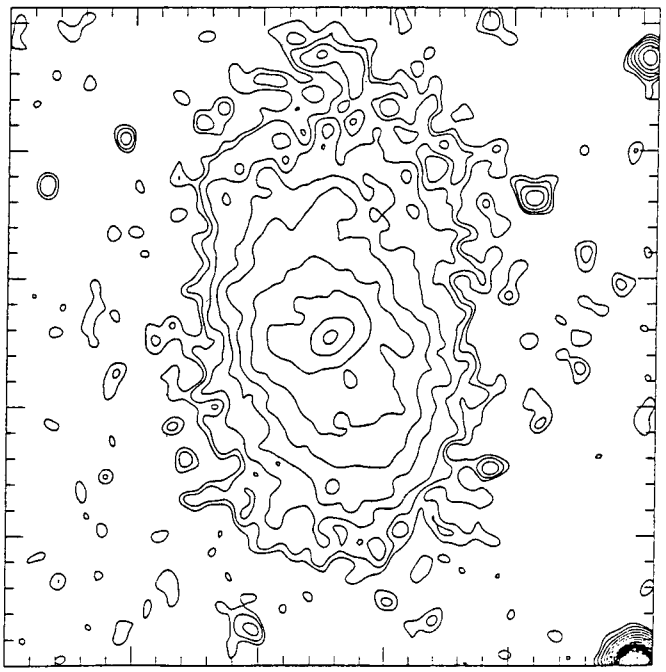

(c)

Fig. 1. Continued: (c) The same for I-band but the surface brightness of the outermost isophote is 3 mag below the sky brightness.

spots which are most pronounced in the B-band image are also observed in the inner ring. Most of these bright spots are thought to be HII regions but the brightest object on the east of the nucleus is too big to be a HII region. It may be a faint foreground or a physical companion galaxy. The horizontally elongated feature in V-band isophote is not a real structure but a defect in the original plate.

The isophotal maps of NGC2715 are presented in Figure 2. Although both of NGC1087 and NGC2715 are classified as SAB(rs)c, there are several differences in the detailed structure of the two galaxies. The nucleus of NGC2715 is extremely faint and the surrounding bulge is smaller than that of NGC1087. There seems to be no sign of a bar crossing the nucleus. Both of the galaxies have inner rings but inner ring of NGC2715 is smoother than that of NGC1087. NGC2715 appears to have two spiral arms which are more pronounced than the multiple spiral arms in NGC1087. Dust lanes are observed along the inner edge of the spiral arms and several HII regions are also observed in the outer parts of the spiral arms.

Figure 3 shows the isophotal maps of NGC2844 which has a very bright bulge. The disk of NGC2844 is relatively small and the spiral arms are not as prominent as those of NGC1087 and NGC2715. No big apparent differences are found between the isophotal maps in different colors except for the I-band one which shows several irregular isophotes in the central parts of the galaxy. These irregular shapes are considered to be due to plate noises.

NGC3593 is a large early type spiral galaxy whose isophotal maps are shown in Figure 4. The bulge of NGC3593 is quite bright but its luminosity does not dominate over the disk luminosity in the outer parts of the galaxy. The luminosity of the disk within 110 arcsec from the nucleus is dominated by the tightly wound spiral arms. Due to overexposures in B plate no structure can be resolved within 5 arcsec from the nucleus.

IV. LUMINOSITY PROFILES AND PROFILE DECOMPOSITION

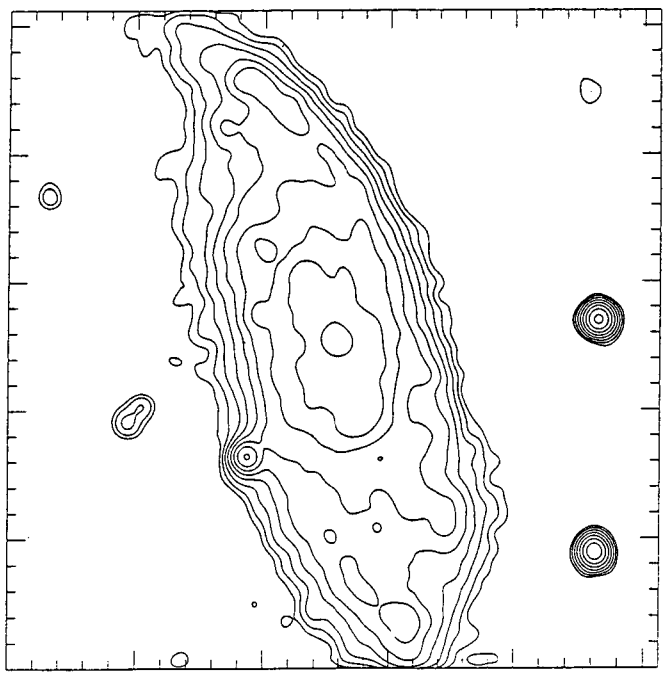

N2715 B

(a)

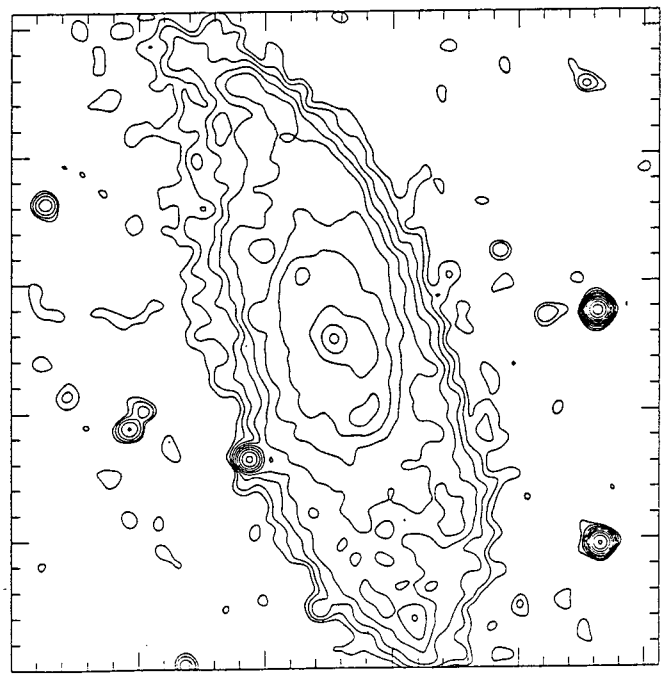

N2715 V

(b)

Fig. 2. Isophotal maps of NGC2715. North is at top and east at left. The intervals of isophotes are 0.5 mag. The mean position angle of spiral arms are similar to that of the the disk. (a) B-band isophotal map. Spiral arms and dust lanes are well observed . The outermost isophote represents 25.5 mag/arcsec^2. (b) The same for V-band. The spiral arms can be seen near the nucleus. The outermost isophote is 24.5 mag/arcsec^2.

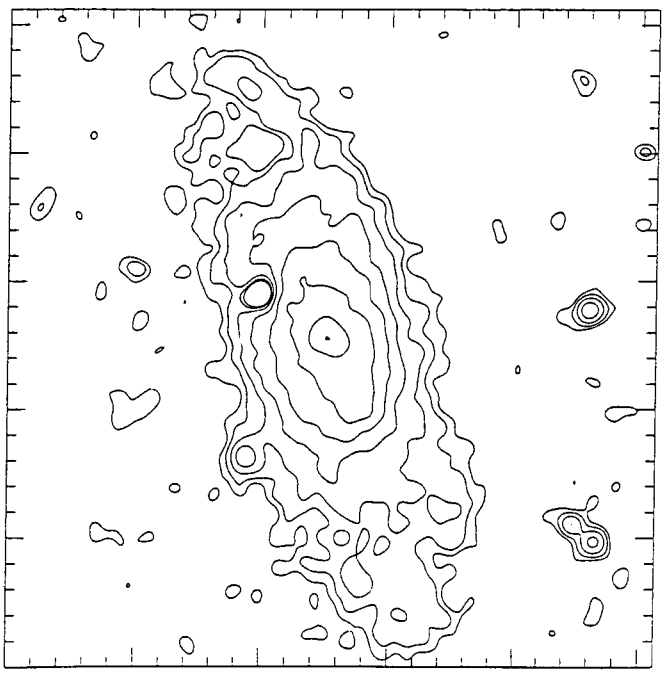

(c)

Fig. 2. Continued: (c) The same for I-band but the surface brightness of the outermost isophote is 3 mag below the sky brightness.

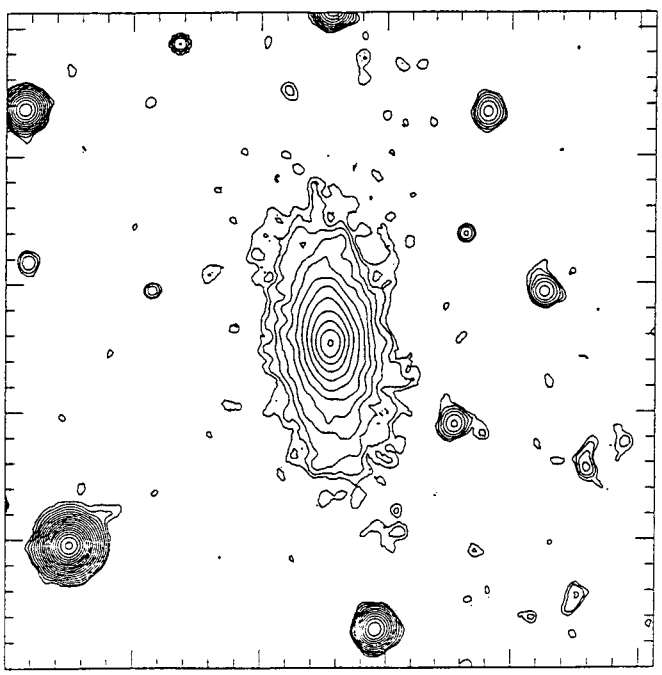

(a)

Fig. 3. Isophotal maps of NGC2844. North is at top and east at left. The intervals of isophotes are 0.5 mag. (a) B-band isophotal map. Spiral arms can be seen. Bulge is very bright and large. The outermost isophote represents 25.5 mag/arcsec^2.

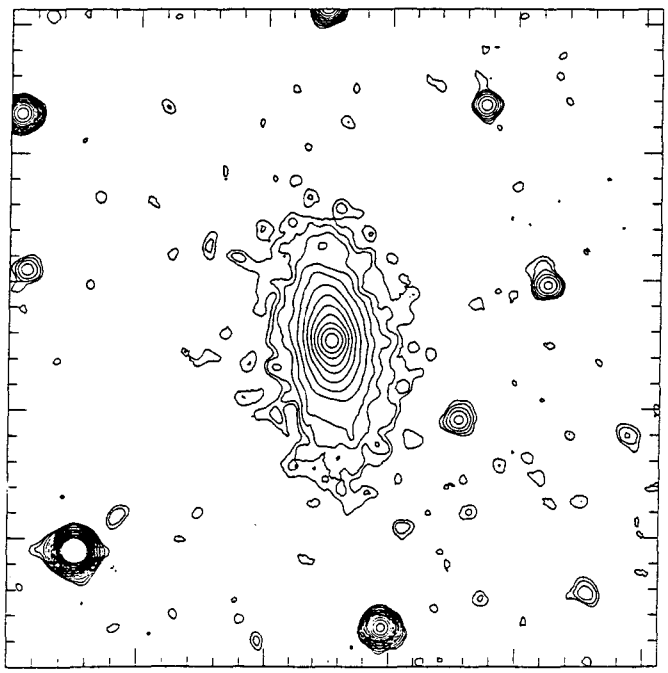

(b)

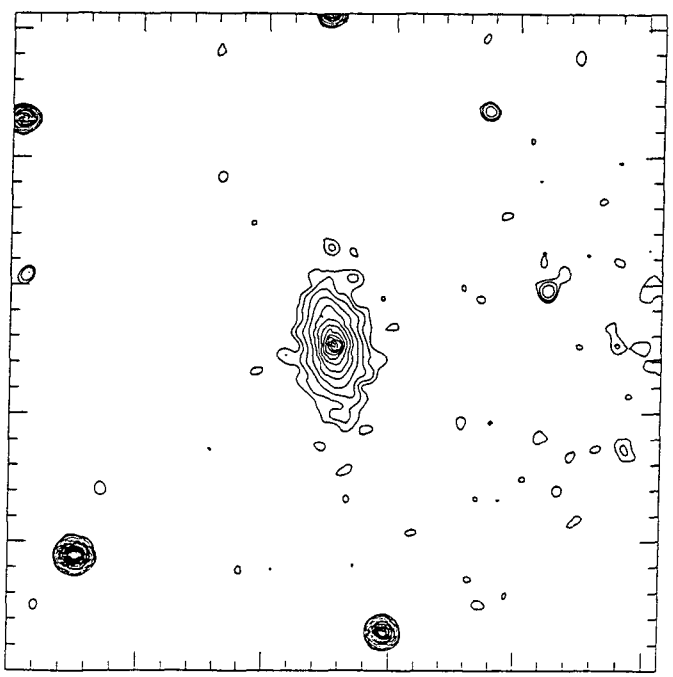

(c)

Fig. 3. Continued: (b) The same for V-band. The contours in the central part are more sircular than those in V-band. The outermost isophote is 24.5 mag/arcsec^2. (c) The same for I-band but the surface brightness of the outermost isophote is 3 mag below the sky brightness. The noisy isophotes near nucleus seems to be caused by the plate noise.

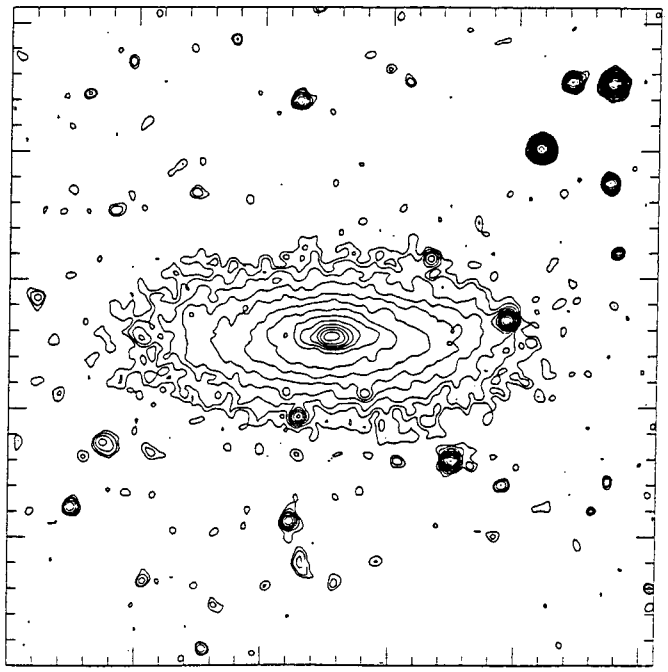

N3593 B

(a)

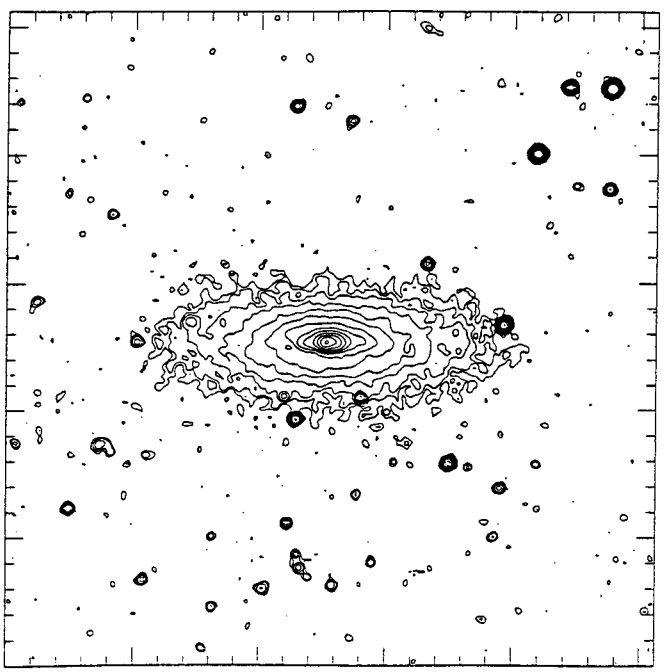

N3593 V

(b)

Fig. 4. Isophotal maps of NGC3593. North is at top and east at left. The intervals of isophotes are 0.5 mag. (a) B-band isophotal map. Spiral arms can be identified easily. The outermost isophote represents 25.5 mag/arcsec^2. (b) The same for V-band. The outermost isophote is 24 mag/arcsec^2.

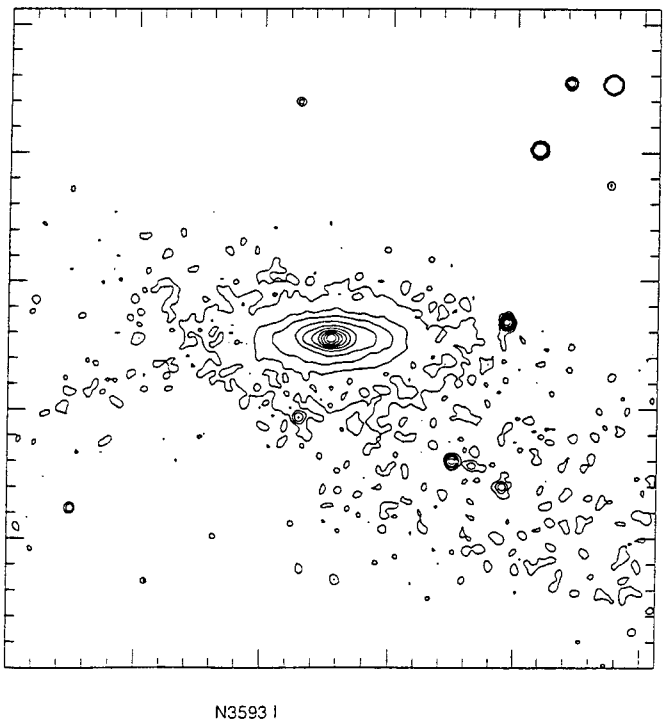

(c)

Fig. 4. Continued: (c) The same for I-band but the surface brightness of the outermost isophote is 1 mag below the sky brightness.

(a) Luminosity Profiles along the Major Axis

The surface brightness distributions along the major axes of NGC1087, NGC2715, NGC2844 and NGC3593 which were derived by fitting the observed isophotes to a series of concentric ellipses are presented in Figure 5. This ellipse fitting technique was developed by Kent (1983) and has been used as a powerful tool to obtain high S/N major axis profiles along with geometric parameters such as position angle (hereafter PA) and ellipticity as shown in Figure 6. The luminosity profiles of four galaxies differ from galaxy to galaxy but all the profiles in Figure 5 show several distinct components such as bulge, disk, spiral arms, etc.

The luminosity profiles of galaxies in different colors look similar but the I-band luminosity profiles are smoother than B- and V-band profiles. The bumps which are most pronounced in the B-band are mainly caused by the spiral arms, but in the case of NGC1087 the bump near $r = 18$ arcsec is due to the inner ring of NGC1087 where several bright HII regions are observed.

The luminosity distribution along the major axis of NGC2715 is much more different from that of NGC1087 whose morphological type is the same as that of NGC2715. The luminosity of NGC2715 declines more slowly than that of NGC1087. The shallow gradient of the luminosity profile of NGC2715 seems to be intrinsic property of the disk of NGC2715. However, the gradient may have been affected by the luminosities from the spiral arms whose mean PA is about 12°.

As shown in Figure 5, the luminosity distribution of NGC2844 is very different from the others. Most of its light comes from the bulge component. The predominant bulge of NGC2844 is more apparent in Figure 7 where the surface brightness distributions are plotted as a function of $r^{1/4}$. Here r is the mean radius which is defined as $r = (ab)^{1/2}$ with a and b being semi-major and semi-minor axes, respectively. The large deviation from the straight line in the central parts of the galaxies is not the intrinsic property of the galaxies but reflects the effects of seeing convolution.

The major axis luminosity profile of NGC3593 in Figure 5 shows a typical luminosity distribution of early type spiral galaxies. The bulge luminosity dominates the inner parts of the galaxy while the disk dominates in the outer parts. The

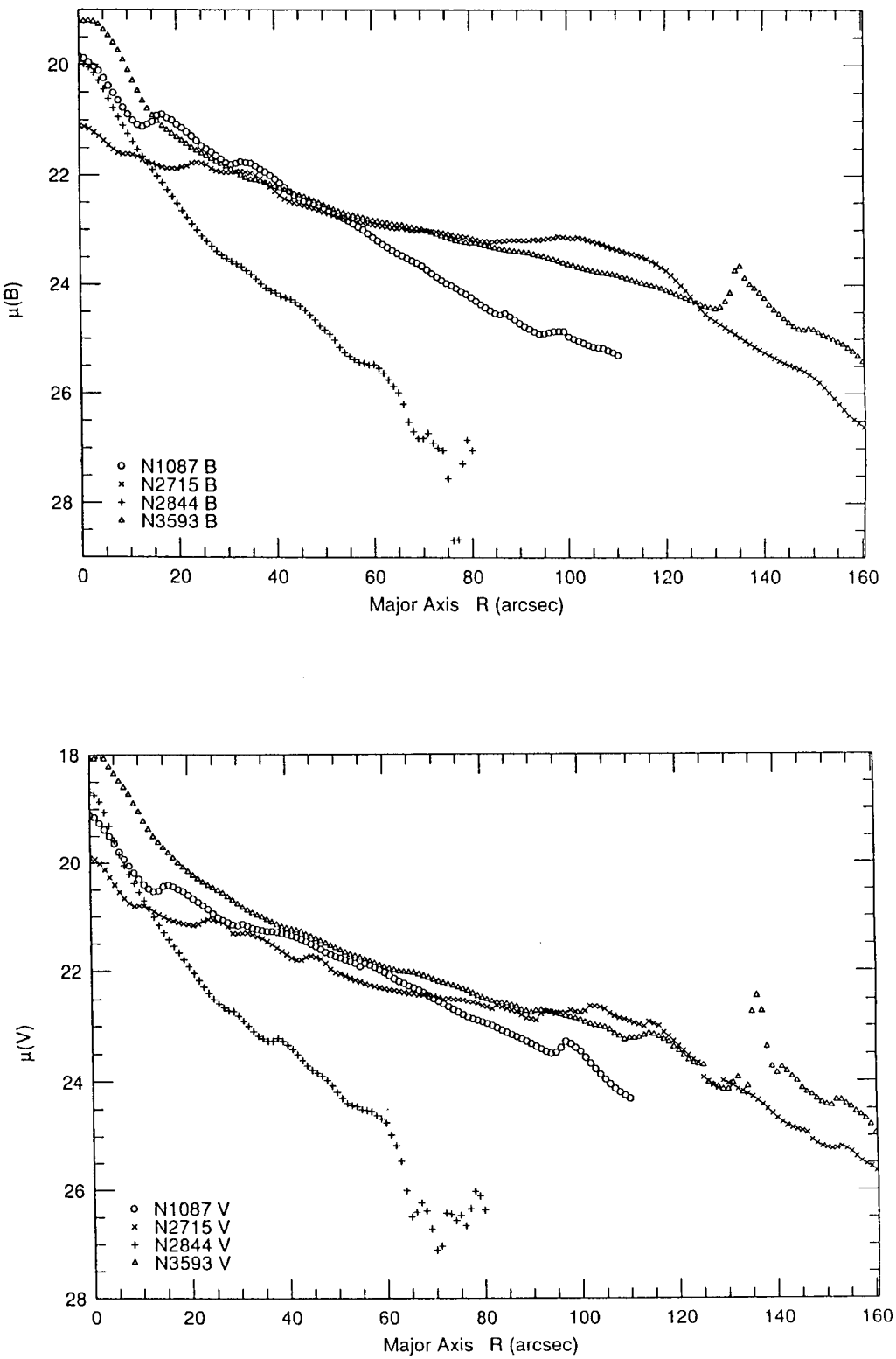

Fig. 5. Surface brightness proflie along the major axes of NGC1087, NGC2715, NGC2844, and NGC3593.

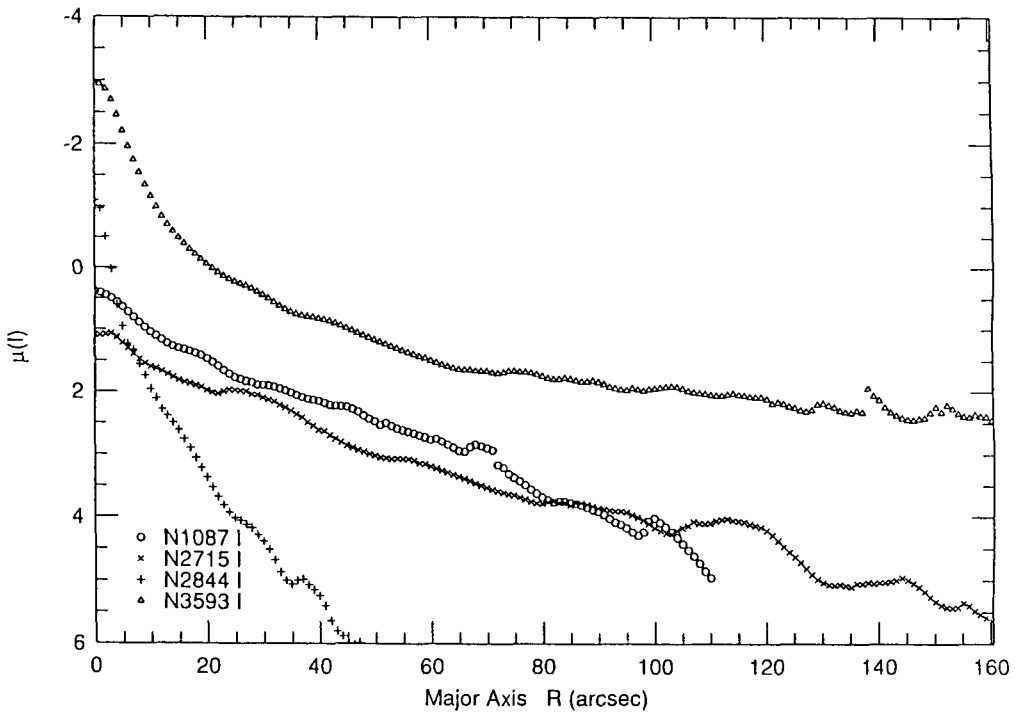

Fig. 5. Continued.

central parts of the B and V profiles show the effects of overexposure.

The PAs and ellipticities of the galaxies as a function of radii along the major axis in Figure 6 are very useful for the examination of the geometrical properties of distinct components. Bulges have small ellipticities which reflect their intrinsic spherical shape. The PAs of the bulge of NGC1087 and NGC2844 are nearly constant while that of NGC3593 varies continuously. The varying PA of the bulge of NGC3593 suggests that the bulge of NGC3593 may be triaxial.

(b) Decomposition of Luminosity Profiles

We tried to decompose the luminosity profiles of the galaxies into disk and bulge components by assuming that the bulge luminosity follows de Vaucouleurs' $r^{1/4}$-law and the disk luminosity follows the exponential law. But it was difficult to decompose the observed luminosity profiles into bulge and disk components except for NGC3593. The failure is considered to be due to the structural properties of these galaxies which cannot be simply decomposed into bulge and disk components.

For NGC1087 and NGC2715, the failure of decomposition is mainly due to the small bulge which does not follow the $r^{1/4}$-law, as shown in Figure 7. In the case of NGC2844 the disk is too faint to be adequately decomposed. One trial decomposition of the I-band luminosity profile of NGC2844 is given in Figure 8 where the bulge luminosity dominates over the disk luminosity. In general, it is easier to decompose the I-band luminosity profiles than B- and V-band profiles. The reason for this is not clear but it is partly due to the fact that I-band is little affected by the dust lanes and the luminosities from the spiral arms.

Figure 9 shows the results of decomposition of the major-axis luminosity profile of NGC3593. The triangles on the abscissa represent the range of radii where observed profiles are fitted to the $r^{1/4}$-law and exponential function. The central surface brightness of the disk of NGC3593 in B-band is 22.05 mag/arcsec^2 which is approximately the same as the mean central surface brightness of disk galaxies (Freeman 1970). It is apparent that the gradient of the disk luminosity profile in I-band is shallower than the gradients of B- and V-band profiles.

V. BRIEF SUMMARY AND CONCLUSIONS

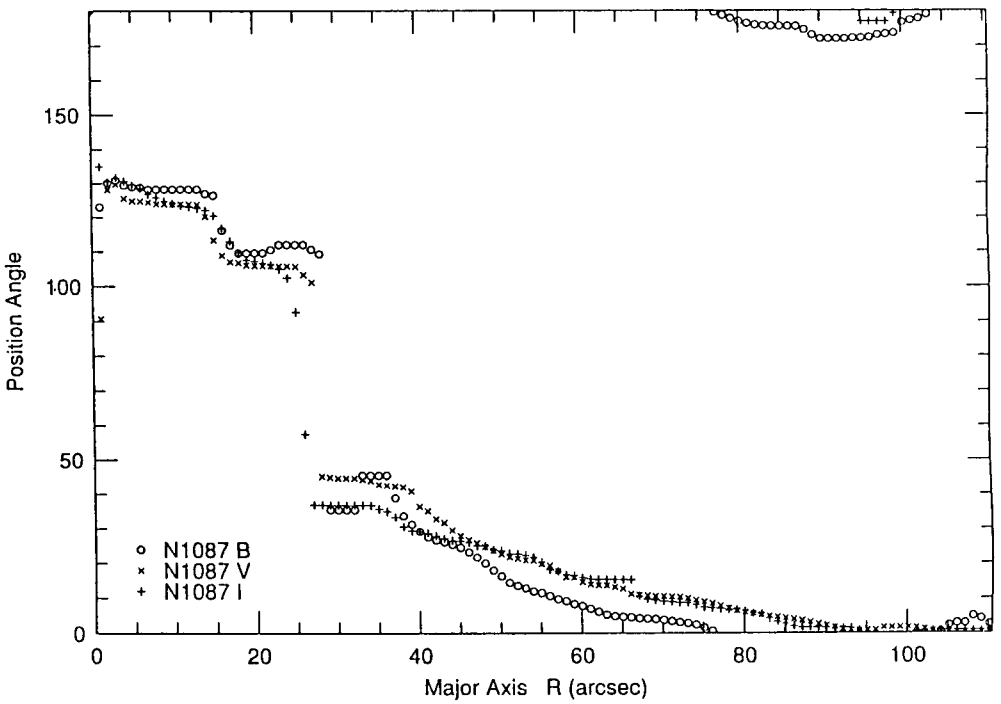

(a)

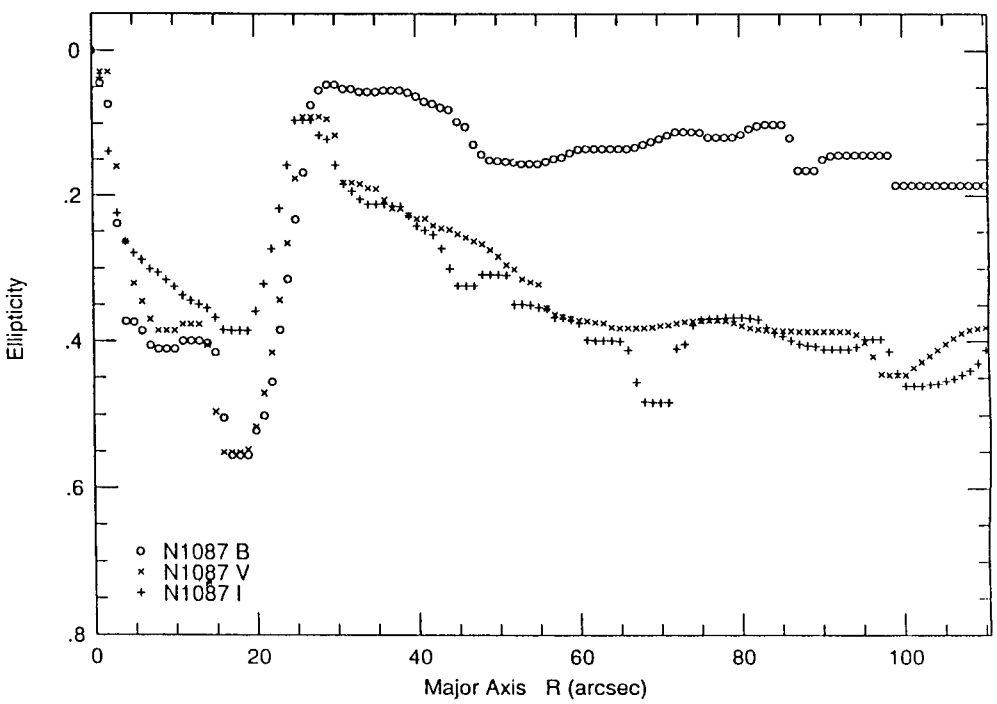

(b)

Fig. 6. Position angles and ellipticities. (a) and (b) for NGC1087.

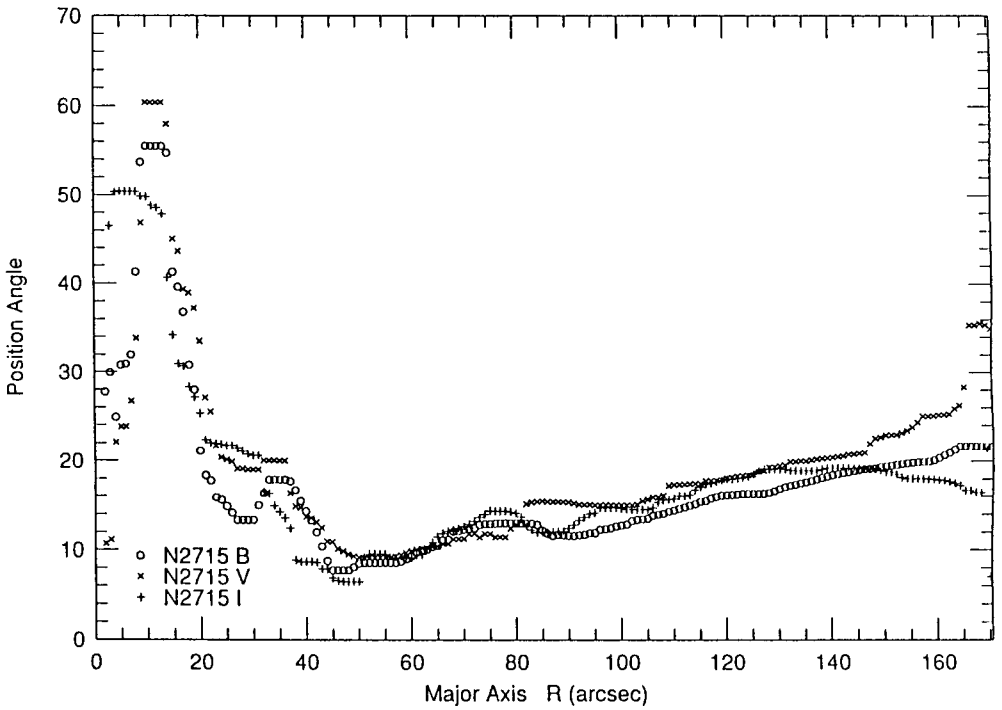

(c)

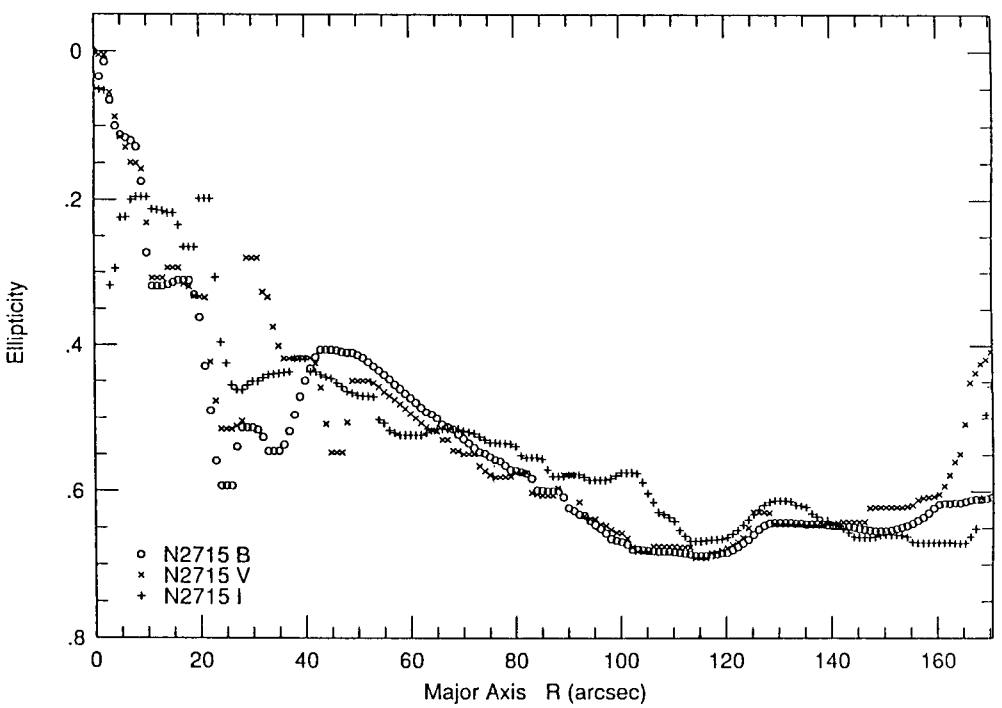

(d)

Fig. 6. Continued: (c) and (d) for NGC2715.

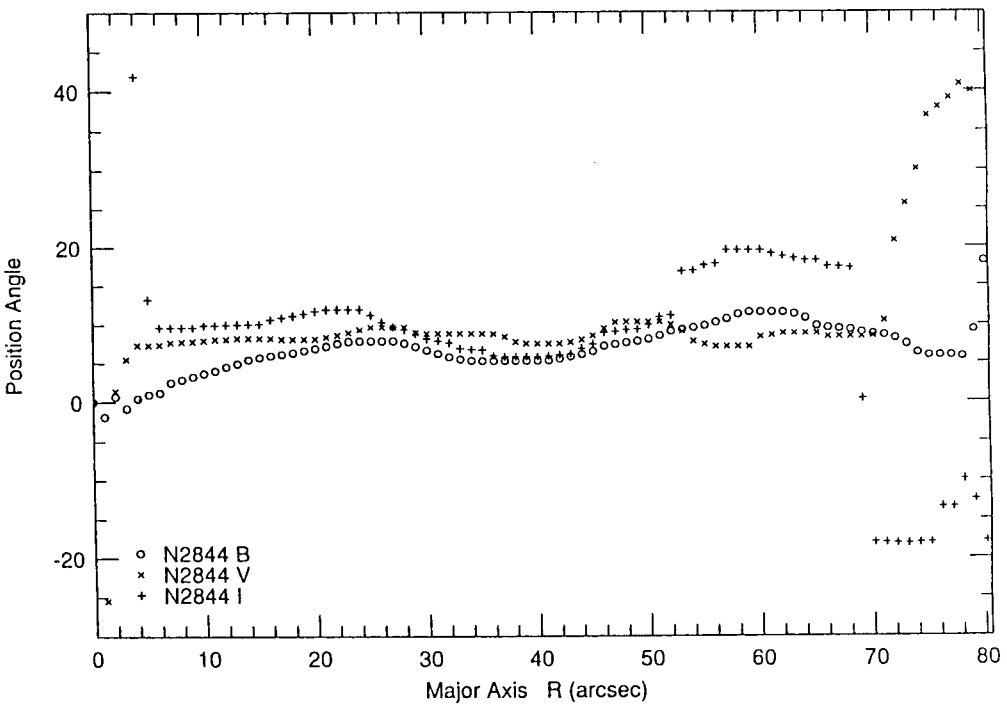

(e)

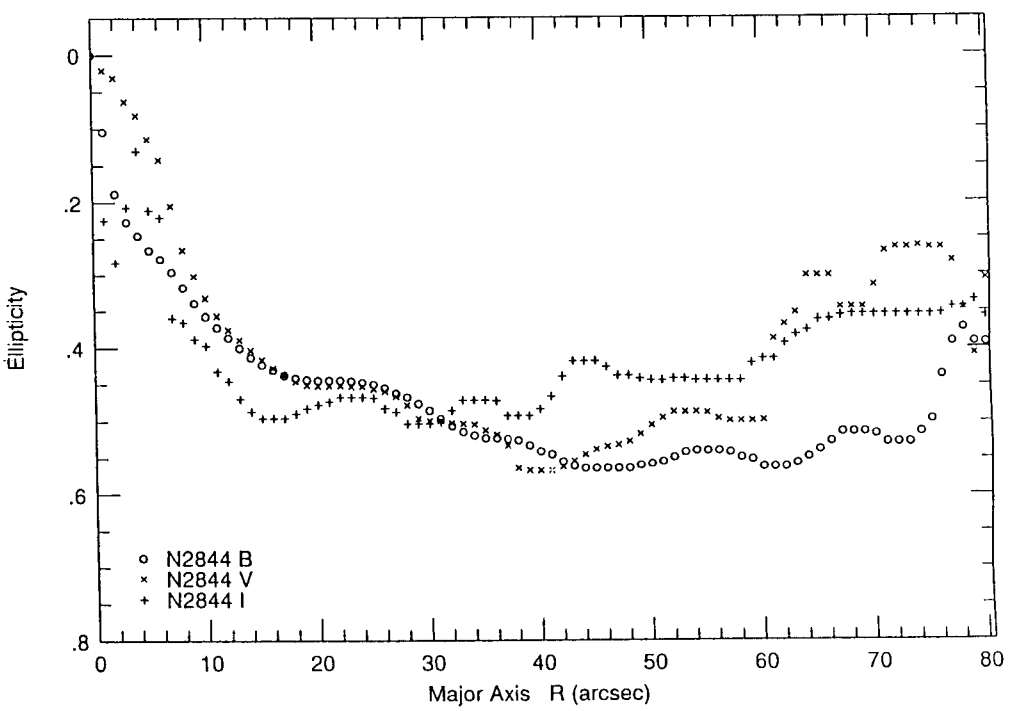

(f)

Fig. 6. Continued: (e) and (f) for NGC2844.

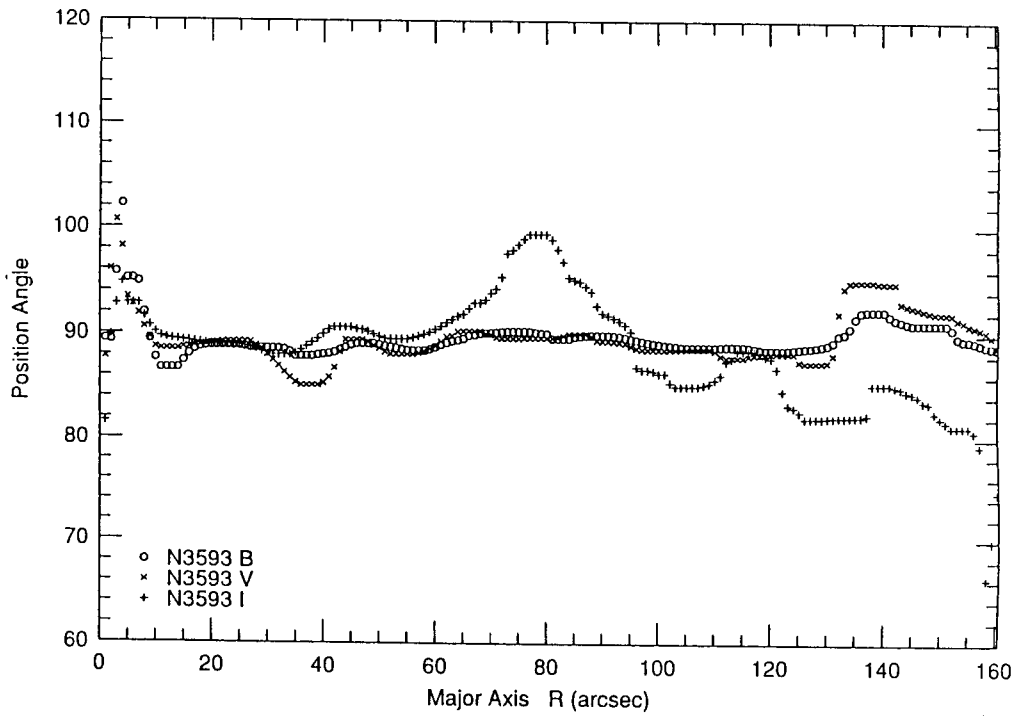

(g)

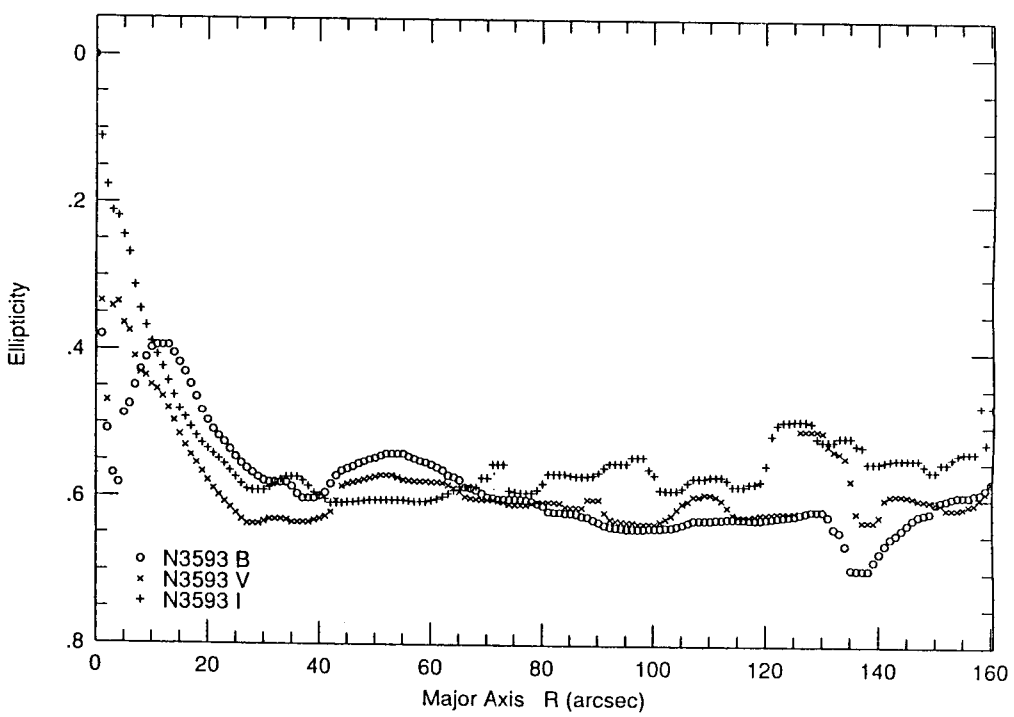

(h)

Fig. 6. Continued: (g) and (h) for NGC3593.

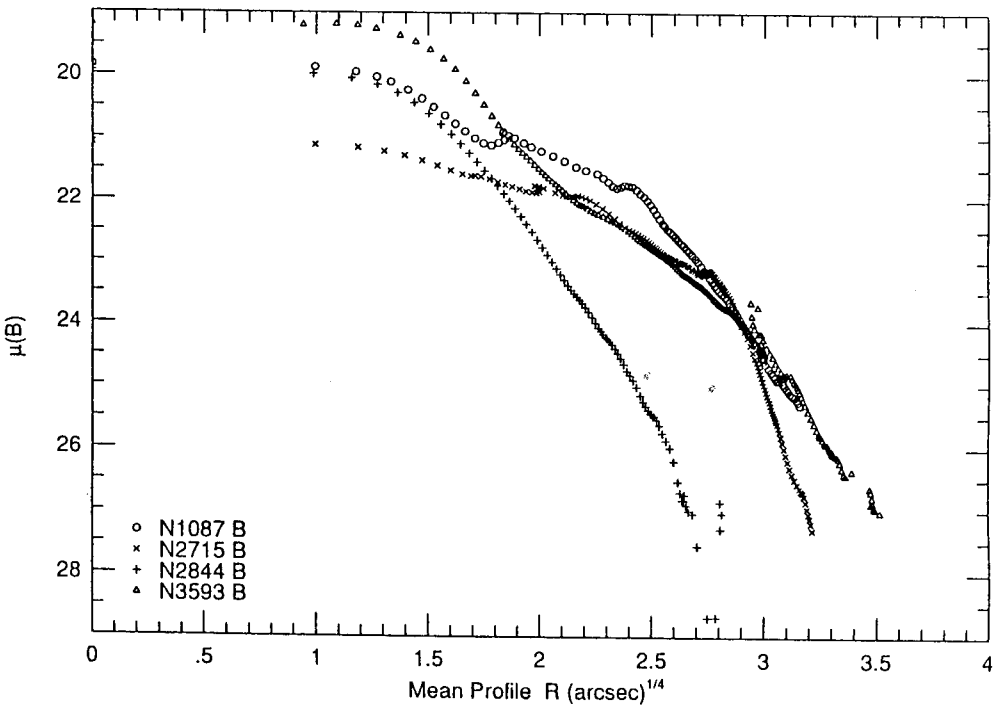

(a)

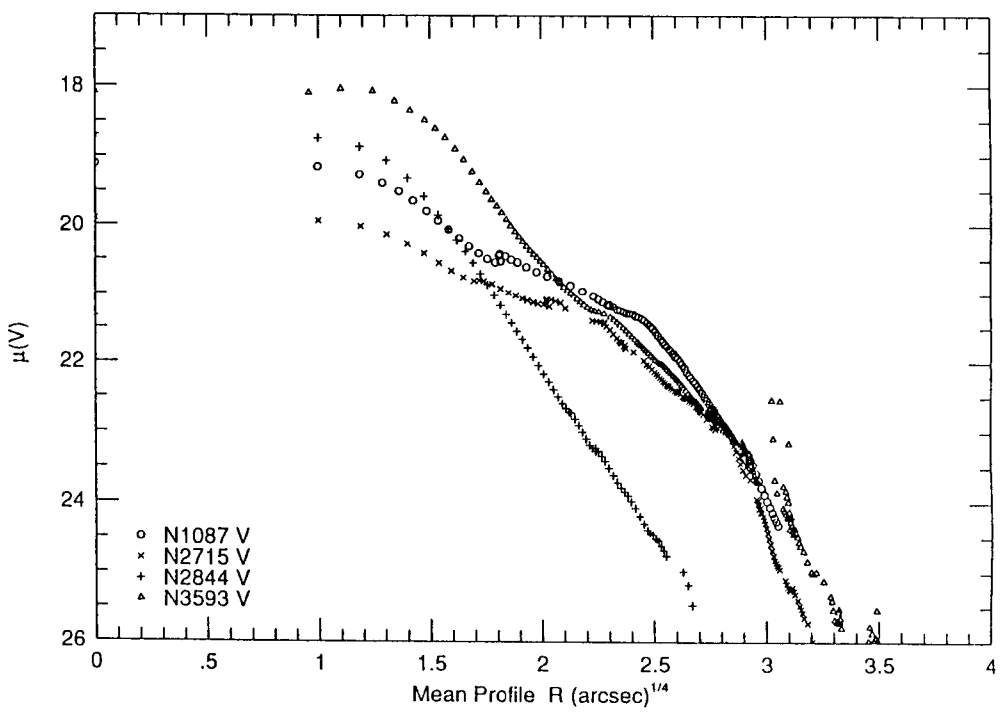

(b)

Fig. 7. Mean surface brightness profiles as a function of $r^{1/4}$. (a) for B-band and (b) for V-band.

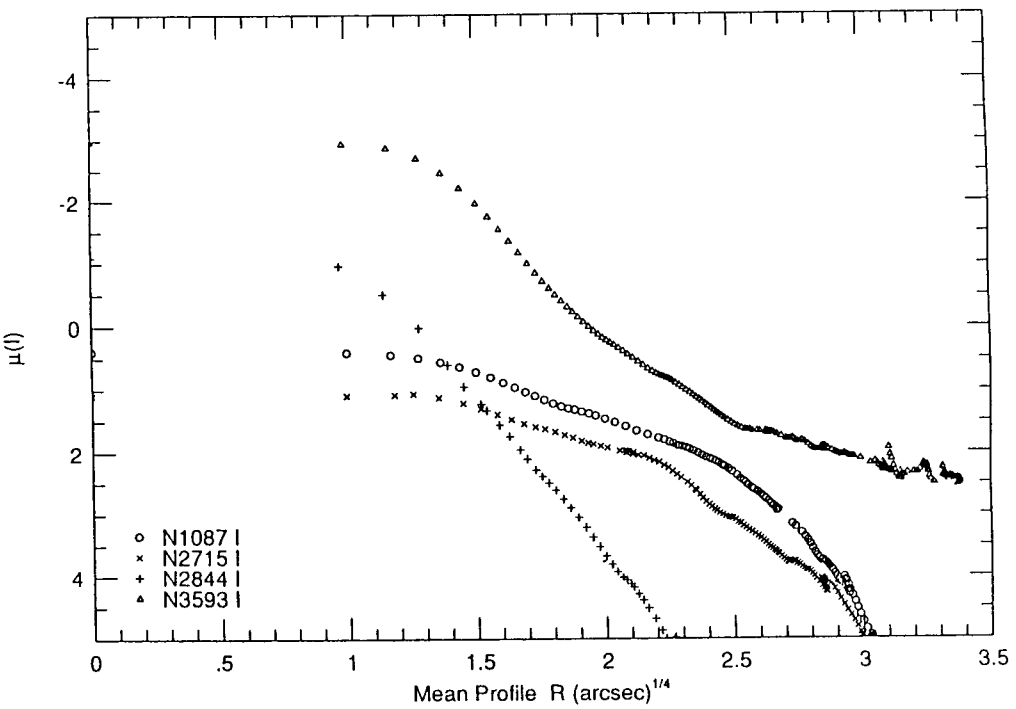

(c)

Fig. 7. Continued: (c) for I-band.

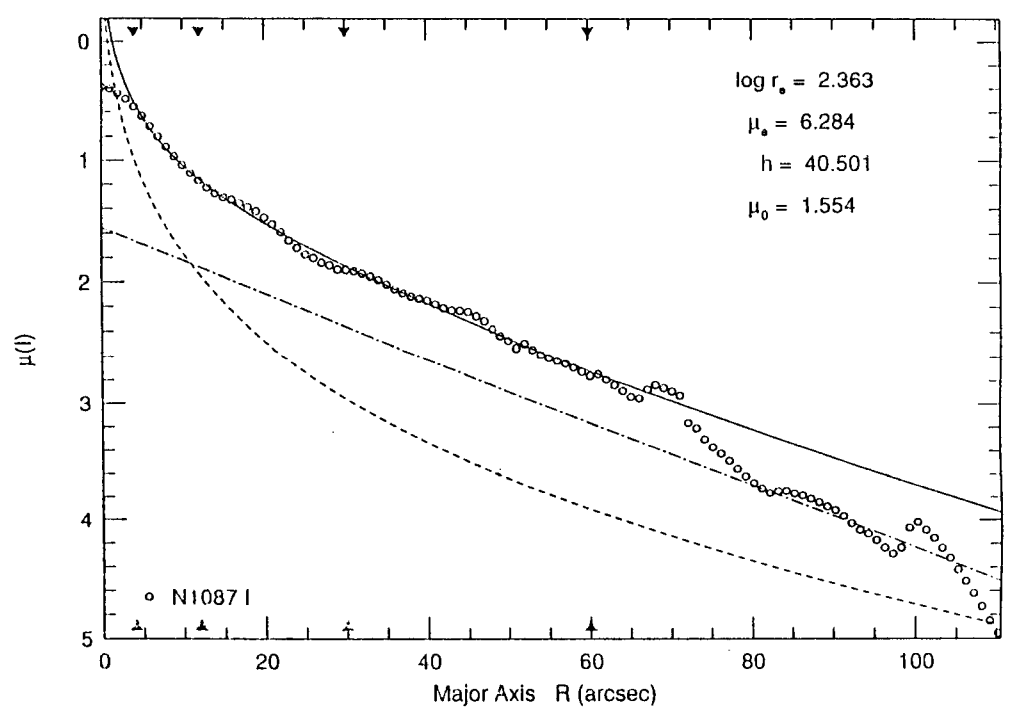

Fig. 8. Decomposition of the luminosity profile of NGC2844 in I-band. Bulge luminosity dominates disk luminosity even in the outer part of the galaxy. The inner two triangles in abscissa represent the fitting range of bulge and the outer two triangles indicate that for disk. The thin solid line represents the combined luminosity of bulge and disk.

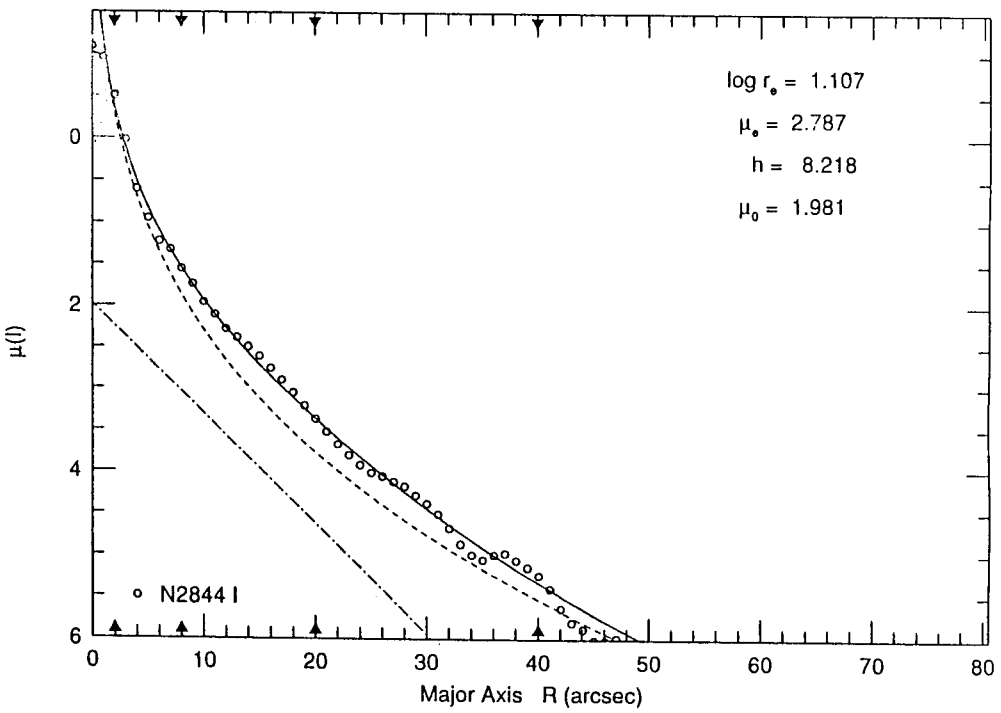

Fig. 9. Decompsition of the luminosity profile of NGC3593. The combined luminosity well fits the observed luminosity distribution.

We examined the morphological properties of four spiral galaxies NGC1087, NGC2715, NGC2844, and NGC3593, by using the BVI Kiso Schmidt plates. All the galaxies in the present study show some peculiarities in their luminosity distributions. Decomposition of the major axis profiles shows that most of the peculiarities are intrinsic to their structures. The luminosity distributions in different colors are not much different except for the fact that spiral arms are more prominent in B-band images.

NGC1087 and NGC2715 have very small nuclei and their bulge luminosities do not follow the $r^{1/4}$-law. The luminosity gradient of the disk of NGC2715 is shallower than that of the other galaxies. Both of NGC1087 and NGC2715 have inner rings but the inner ring of NGC1087 is more prominent due to several bright HII regions. Near the inner ring of NGC1087 a very bright object which seems to be a faint foreground galaxy or a companion was found to exist. But it is not clear whether it is a physical companion galaxy.

An early type galaxy NGC2844 has a very large bulge whose luminosity dominates the disk luminosity even in the outer parts of the galaxy. The major axis profile of NGC2844 is much different from that of NGC3593 whose morphological type is similar. Detailed profile decomposition showed that bulge luminosity dominates over the disk luminosity in all the radii. NGC3593 seems to be a typical early type spiral. Its luminosity profiles were well decomposed into bulge and disk components. The central surface brightness of the disk of NGC3593 is very similar to the mean central surface brightness of Freeman disk.

ACKNOWLEDGEMENTS

This research was supported in part by the Korea Science and Engineering Foundation and Korea Astronomy Observatory. We are grateful to the staff of Kiso Astronomical Observatory for providing plate materials for the present study. H.B. Ann thanks to the hospitalities of DAO where the draft of this paper were prepared.

REFERENCES

Ann, H. B., 1986, J. Kor. Astron. Soc., 19., 69
Ann, H. B., 1987, J. Kor. Astron. Soc., 20., 49
Ann, H. B., 1993, in preparation
Freeman, K. C., 1970, ApJ, 160, 811
Hamabe, M., 1992, private communications
Ichikawa, S., Okamura, S., Watanabe, M., Hamabe, M., Aoki, T., & Kodaira, K., 1987, Annals Tokyo Astron. Obs., 21, 185
Kent, S. M., 1983, ApJ, 266, 562
Kodaira, K., Okamura, S., & Ichikawa, S., 1990, Photometric Atlas of Northern Bright Galaxies(Univ. of Tokyo Press: Tokyo)
Longo, G., & de Vaucouleurs, G. A., 1983, A General Catalogue of Photoelectric Magnitudes and Colors in the UBV Systems(U. of Texas Press: Austin, TX)
Mihalas, D., & Binney, J., 1981, Galactic Astronomy(W. H. Freeman and Co.; San Francisco), Chap. 5
Okamura, S., 1988, PASP, 100, 524
Okamura, S., Kodaira, K., & Watanabe, M., 1984, ApJ, 180, 7
Tarusawa, K., Soyano, T., Noguchi, T., & Okamura, S., 1986, Tokyo Astron. Obs. Report, 20, 674
Watanabe, M., Kodaira, K., & Okamura, S., 1982, ApJS, 50, 1
Watanabe, M., Kodaira, K., & Okamura, S., 1985, ApJS, 292, 72